Adaptive Mode Selection and Power Allocation for D2D Underlay Cellular Networks with Dynamic Fading Channel

Mengwei Sun, Yuan Ding, *Member, IEEE,* George Goussetis, *Senior Member, IEEE*

***Abstract*—This paper studies the adaptive mode selection and power allocation for D2D underlay cellular communication systems with the consideration of dynamic fading channel state information (CSI). It aims to maximize the throughput of D2D users while guaranteeing the required quality of service (QoS) of cellular networks. To solve this problem, the expression of throughput for D2D users under dynamic CSI is firstly derived. Subsequently, an adaptive mode selection and power allocation scheduling are obtained. Numerical simulations are provided to validate the analysis and throughput enhancement.**

***Index Terms*—D2D underlay network, dynamic fading channel, mode selection, power allocation.**

I. Introduction

Device-to-Device (D2D) [1], [2] communications enable multiple mobile users in proximity to directly transfer signals/information, which is a promising solution to accommodating high data demands of mobile users and enhancing network spectral efficiency. There are two common modes that can be selected for underlay D2D communications: regular cellular mode and D2D underlay mode [2]. Previous works on mode selection focused on joint mode selection and power allocation scheme assuming that perfect instantaneous channel state information (CSI) is fully known [3]-[5]. This assumption does not hold in some important application scenarios, e.g. mobile or dynamic environments. Lately, a power allocation scheme was proposed [6] based on the statistical CSI, i.e., the *a priori* probability density function (PDF). However, this approach ignores the underlying correlation property of the dynamic CSI and hence become less attractive. As far as the authors are aware, the dynamical mode selection and power allocation schedule in time varying fading (TVF) channels remains unexplored.

In this paper, we introduce a hybrid mode selection with adaptive power allocation scheduling. First, the optimization problem is formulated as a dynamic throughput maximization problem considering TVF D2D links. Then, the theoretical analysis revealing relations between optimal power allocation and the D2D channel gain is performed. Finally, the adaptive scheduling with channel estimation algorithm is developed.

II. System Model

This paper studies an underlay cellular network consisting of a cellular base station (CBS), a cellular user equipment (CUE), a D2D transmitter (DT), and a D2D receiver (DR), as shown in Fig. 1. Under hybrid mode, the DT multicasts its messages to DR via two links, i.e., a direct link and a relay link. The relay link refers to that the DT transmits the message to CBS in the uplink session and then the CBS conveys the message to DR in the downlink session. The D2D direct link shares the same time-frequency resources with the cellular users. The bandwidth is assumed to be W. The relay link participates in the cellular uplink session with the CUE, and the spectrum access rate is set to be β, and $0 \leq \beta \leq 1$ [6]. Specifically, the spectrum of the CBS is divided into B frequency sub-bands, i.e., $W = \sum_B w$, and D2D users can independently access βB of them. The allocated transmitted power for these two links is set to be ξP_D and $(1-\xi)P_D$ respectively, where $0 \leq \xi \leq 1$. Note, when $\xi = 0$, the hybrid mode becomes the regular cellular mode, while when $\xi = 1$, it is the direct D2D mode.

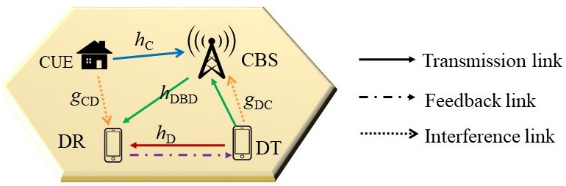

Fig. 1: Hybrid mode in underlay cellular network.

The channel gain from the CUE to the CBS, the direct D2D link, and the relay link are denoted as h_C, h_D and h_{DBD} respectively. The interference channels between the cellular and D2D networks are represented as g_{CD} and g_{DC} respectively. For most emerging D2D applications involving mobile devices (e.g., LTE-A) [7] or some specific environments with relative movements (e.g., indoor offices), the fading gain between D2D users becomes a time-varying random process. In this paper, the distribution of the channel amplitude is set as Rician fading, and its evolution is modelled using the first-order finite-state Markov chain (FSMC) [8]. Specifically, the fading amplitude is discrete into K states, i.e., $|h_D(n)| \in \mathcal{A} = \{A_0, A_1, \cdots, A_{K-1}\}$ and evolves according to the first-order Markov process with the transition probability matrix (TPM) Γ, i.e., $\Pr\left(|h_D(n)| = A_i \mid |h_D(n-1)| = A_j\right) = \Gamma_{j,i}$. $\Gamma_{j,i}$ relate only to the channel amplitude PDF and states number [8], and hence can be treated as static and used as *a priori* information.

III. Problem Formulation and Analysis

The optimization objective for the mode selection and power allocation is to maximize the achievable average throughput

M. W. Sun is with the University of Edinburgh, Edinburgh, EH9 3FG, UK (msun@ed.ac.uk). Y. Ding and G. Goussetis are with the Heriot-Watt University, Edinburgh, EH14 4AS, UK (yuan.ding@hw.ac.uk; g.goussetis@hw.ac.uk

The work was supported by the EPSRC (UK) under Grant EP/P025129/1 and EP/V002635/1.

of the D2D network while guaranteeing the minimum QoS of the CUE, which can be formulated as:

$$\max_{0\le\xi\le 1} \; U(\xi,\beta,h_D), \tag{1}$$

$$\textbf{s.t.} \quad SINR_C \ge \lambda_C. \tag{2}$$

where the achievable average throughput U and SNIR for the CUE can be calculated by:

$$U(\xi,\beta,h_D) = \frac{1}{N}\sum_{n=0}^{N-1} u(\xi(n),\beta,h_D(n)), \tag{3}$$

$$SNIR_C(n) = 10\log_{10}\left(\frac{P_C|h_C|^2}{\xi(n)P_D|g_{DC}|^2+\sigma^2}\right). \tag{4}$$

Here, n is the index of time slot and its length is set to be N. β is the spectrum access rate for the relay link which was defined in Section I. $\xi(n)$ is the allocated power rate for the D2D direct link at n-th time slot. P_C is the emitted power of CUE and σ^2 is the variance of channel noise assumed to be zero-mean additive white Gaussian noise (AWGN). Substituting (4) into (2) yields the range for $\xi(n)$, i.e., $\xi(n) \in \left[0, \min\left(1, \frac{P_C|h_C|^2-\sigma^2\lambda^\dagger}{\lambda^\dagger P_D|g_{DC}|^2}\right)\right]$, where $\lambda^\dagger = 10^{\frac{\lambda_C}{10}}$. Therefore, the maximization problem in (1) and (2) can be rewritten as:

$$\max_{0\le\xi(n)\le 1} \; u(\xi(n),\beta,h_D(n)), \; n = 0,\ldots,N-1, \tag{5}$$

$$\textbf{s.t.} \quad 0 \le \xi(n) \le \min\left(1, \frac{P_C|h_C|^2-\sigma^2\lambda^\dagger}{\lambda^\dagger P_D|g_{DC}|^2}\right). \tag{6}$$

There are two links that contribute to the throughput of the D2D network, i.e., the data transmission via the D2D direct link and the CBS relay link, see (7),

$$\begin{aligned} u(\xi(n),\beta,h_D(n)) &= u_{DD}(n) + u_{DBD}(n) \\ &= W\log_2\left(1+\frac{\xi(n)P_D|h_D(n)|^2}{P_C|g_{CD}|^2+\sigma^2}\right) \\ &\quad + \beta W\log_2\left(1+\frac{(1-\xi(n))P_D|h_{DBD}|^2}{\sigma^2}\right). \end{aligned} \tag{7}$$

The first partial derivative of $u(\xi(n),\beta,h_D(n))$ with respect to $\xi(n)$ can be derived as:

$$\begin{aligned} F(\xi(n),\beta,h_D(n)) &= \frac{\partial u(\xi(n),\beta,h_D(n))}{\partial \xi(n)} \\ =& W\frac{1}{\ln 2\left(1+\frac{\xi(n)P_D|h_D(n)|^2}{P_C|g_{CD}|^2+\sigma^2}\right)}\frac{P_D|h_D(n)|^2}{P_C|g_{CD}|^2+\sigma^2} \\ &-\beta W\frac{1}{\ln 2\left(1+\frac{(1-\xi(n))P_D|h_{DBD}|^2}{\sigma^2}\right)}\frac{P_D|h_{DBD}|^2}{\sigma^2} \\ =&\frac{WP_D}{\ln 2}\left[\frac{|h_D(n)|^2}{P_C|g_{CD}|^2+\sigma^2+\xi(n)P_D|h_D(n)|^2}\right. \\ &\left.-\frac{\beta|h_{DBD}|^2}{\sigma^2+(1-\xi(n))P_D|h_{DBD}|^2}\right]. \end{aligned} \tag{8}$$

$$\begin{aligned} &\lim_{\xi(n)\to 0} F(\xi(n),\beta,h_D(n)) \\ &= \frac{WP_D}{\ln 2}\times\left[\frac{|h_D(n)|^2}{P_C|g_{CD}|^2+\sigma^2}-\frac{\beta|h_{DBD}|^2}{\sigma^2+P_D|h_{DBD}|^2}\right], \end{aligned} \tag{9}$$

$$\begin{aligned} &\lim_{\xi(n)\to 1} F(\xi(n),\beta,h_D(n)) \\ &= -\frac{WP_D}{\ln 2}\times\left[\frac{\beta|h_{DBD}|^2}{\sigma^2}-\frac{|h_D(n)|^2}{P_C|g_{CD}|^2+\sigma^2+P_D|h_D(n)|^2}\right]. \end{aligned} \tag{10}$$

Results associated with different channel states are shown in Table I. The second order partial derivative of $u(\xi(n),\beta,h_D(n))$ with respect to $\xi(n)$ can be derived as:

$$\begin{aligned} \frac{\partial^2 u(\xi(n),\beta,h_D(n))}{\partial \xi(n)^2} &= \frac{\partial F(\xi(n),\beta,h_D(n))}{\partial \xi(n)}, \\ = -\frac{WP_D^2}{\ln 2}&\left\{\frac{|h_D(n)|^4}{\left[P_C|g_{CD}|^2+\sigma^2+\xi(n)P_D|h_D(n)|^2\right]^2}\right. \\ &\left.+\frac{\beta|h_{DBD}|^4}{\left[\sigma^2+(1-\xi(n))P_D|h_{DBD}|^2\right]^2}\right\} < 0. \end{aligned} \tag{11}$$

We can conclude from (11) that the first partial derivative $F(\xi(n),\beta,h_D(n))$ is monotonically decreasing with respect to $\xi(n)$. With the conclusions shown in Table I, we have the following theorems.

Theorem 1: $u(\xi(n),\beta,h_D(n))$ is concave in $\xi(n)$ under the Condition $\{1,1\}$ and the Condition $\{2,1\}$, Thus, the maximum point of $u(\xi(n),\beta,h_D(n))$ will be unique in the range $\xi(n) \in [0,1]$ for any chosen $h_D(n)$. In this case, the hybrid mode will be selected and the optimal allocation power denoted as $\xi(n)^\dagger$ is shown in (12).

Theorem 2: $F(\xi(n),\beta,h_D(n))$ is a constant greater than 0 under Condition $\{2,2\}$ which implies that $u(\xi(n),\beta(n),h_D(n))$ is monotonically increasing. Hence, under the Condition $\{2,2\}$, $\xi(n)^\dagger = \min\left(1, \frac{P_C|h_C|^2-\sigma^2\lambda^\dagger}{\lambda^\dagger P_D|g_{DC}|^2}\right)$. If $\frac{P_C|h_C|^2-\sigma^2\lambda^\dagger}{\lambda^\dagger P_D|g_{DC}|^2} \ge 1$, the D2D mode will be adopted, otherwise the hybrid mode will be selected with the power allocation $\xi(n)^\dagger = \frac{P_C|h_C|^2-\sigma^2\lambda^\dagger}{\lambda^\dagger P_D|g_{DC}|^2}$.

Theorem 3: $F(\xi(n),\beta,h_D(n))$ is a constant less than 0 under the Condition $\{1,2\}$ and the Condition $\{2,3\}$ which implies that $u(\xi(n),\beta,h_D(n))$ is monotonically decreasing. Hence, the regular cellular mode, i.e., $\xi(n)^\dagger = 0$, is optimal when $|h_D(n)|^2 < \frac{\beta\left(P_C|g_{CD}|^2+\sigma^2\right)|h_{DBD}|^2}{\sigma^2+P_D|h_{DBD}|^2}$.

IV. Procedure of Adaptive Power Allocation Scheduling

In order to accomplish the adaptive power allocation scheduling premised on the above reconfiguration relation theorems, the channel gain estimation needs to be performed at DR and fed back to the DT.

1) Channel estimation at DR

The channel estimation can be performed after the observation signal $y(n)$ received via maximum *a posteriori* probability (MAP) criterion [9],

$$\begin{aligned} &|\hat{h}_D(n)| \\ &= \arg\max_{|h_D(n)|\in\mathcal{A}} p\left(|h_D(n)| \mid y(n), |\hat{h}_D(n-1)|, \Psi\right), \\ &= \arg\max_{|h_D(n)|\in\mathcal{A}} p\left(y(n) \mid |h_D(n)|, \Psi\right) p\left(|h_D(n)| \mid |\hat{h}_D(n-1)|\right). \end{aligned} \tag{13}$$

where $\Psi = \left\{h_{DBD}, g_{CD}, \xi(n)^\dagger, P_D, P_C, \sigma^2\right\}$. The estimated channel gain of D2D link $|\hat{h}_D(n)|$ is then fed back to DT via feedback link, as shown in Fig. 1.

2) Transmission power allocation determination

TABLE I: The first partial derivative of $u(\xi, \beta, h_D)$

Condition I	Condition II	Results
$\beta P_D \lvert h_{DBD}\rvert^2 > \sigma^2$	$\lvert h_D\rvert^2 > \frac{\beta\left(P_C\lvert g_{CD}\rvert^2+\sigma^2\right)\lvert h_{DBD}\rvert^2}{\sigma^2+P_D\lvert h_{DBD}\rvert^2}$, i.e., Condition $\{1,1\}$	$F(\xi=0)>0, F(\xi=1)<0$
	$\lvert h_D\rvert^2 < \frac{\beta\left(P_C\lvert g_{CD}\rvert^2+\sigma^2\right)\lvert h_{DBD}\rvert^2}{\sigma^2+P_D\lvert h_{DBD}\rvert^2}$, i.e., Condition $\{1,2\}$	$F(\xi=0)<0, F(\xi=1)<0$
$\beta P_D \lvert h_{DBD}\rvert^2 < \sigma^2$	$\frac{\beta\left(P_C\lvert g_{CD}\rvert^2+\sigma^2\right)\lvert h_{DBD}\rvert^2}{\sigma^2+P_D\lvert h_{DBD}\rvert^2} < \lvert h_D\rvert^2 < \frac{\beta\left(P_C\lvert g_{CD}\rvert^2+\sigma^2\right)\lvert h_{DBD}\rvert^2}{\sigma^2-\beta P_D\lvert h_{DBD}\rvert^2}$, i.e., Condition $\{2,1\}$	$F(\xi=0)>0, F(\xi=1)<0$
	$\lvert h_D\rvert^2 > \frac{\beta\left(P_C\lvert g_{CD}\rvert^2+\sigma^2\right)\lvert h_{DBD}\rvert^2}{\sigma^2-\beta P_D\lvert h_{DBD}\rvert^2}$, i.e., Condition $\{2,2\}$	$F(\xi=0)>0, F(\xi=1)>0$
	$\lvert h_D\rvert^2 < \frac{\beta\left(P_C\lvert g_{CD}\rvert^2+\sigma^2\right)\lvert h_{DBD}\rvert^2}{\sigma^2+P_D\lvert h_{DBD}\rvert^2}$, i.e., Condition $\{2,3\}$	$F(\xi=0)<0, F(\xi=1)<0$

$$\xi(n)^{\dagger} = \min\left[\frac{\sigma^2|h_D(n)|^2 + P_D|h_{DBD}|^2|h_D(n)|^2 - \beta P_C|g_{CD}|^2|h_{DBD}|^2 - \beta\sigma^2|h_{DBD}|^2}{(1+\beta)\,P_D|h_{DBD}|^2|h_D(n)|^2}, \frac{P_C|h_C|^2 - \sigma^2\lambda^{\dagger}}{\lambda^{\dagger}P_D|g_{DC}|^2}\right],$$
$$\textbf{s.t.}\quad \text{Condition}\,\{1,1\}\,,\quad \text{Condition}\,\{2,1\}\,. \tag{12}$$

The predictive channel gain is achieved at DT based on its Markov characteristic and the previous estimation results, i.e., $|\hat{h}_D(n|n+1)| = \arg\max_{|h_D(n+1)|\in\mathcal{A}} p\left(|h_D(n+1)|\,|\,|\hat{h}_D(n)|\right)$. By comparing $|\hat{h}_D(n|n+1)|$ with different thresholds shown in Table I, the Condition$\{\cdot,\cdot\}$ is specified. Then, optimum power allocation $\xi(n+1)^{\dagger}$ can be performed based on the specified Condition $\{\cdot,\cdot\}$ and the Theorem 1 to Theorem 3.

3) Implementation

The schematic implementation of the new adaptive scheduling is illustrated in Fig. 2. The allocated power ratio in the transmission slot is adjusted firstly according to the predictive channel state and the proposed reconfiguration relation theorems. Then, the observation signal at the D2D receiver is used for the channel estimation relying on the MAP criterion.

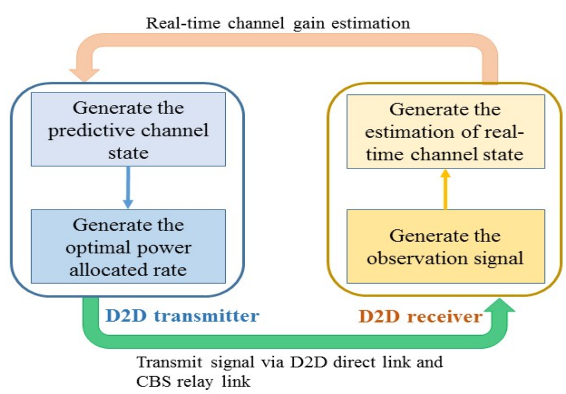

Fig. 2: Implementation of the proposed adaptive switch scheduling.

V. Numerical Results and Discussions

In this section, simulation results and discussions are presented to evaluate the system throughput achieved by the proposed scheduling.

We first show the joint impact of the allocated power rate ξ and the channel gain of the D2D link $|h_D|$ on the first partial derivative of achievable throughput of D2D users, i.e., $F(\xi, \beta, h_D)$. It can be observed from Fig. 3 that,

<u>*Remark 1*</u>: $F(\xi, \beta, h_D)$ is monotonically decreasing in ξ within the range $\xi \in [0, 1]$.

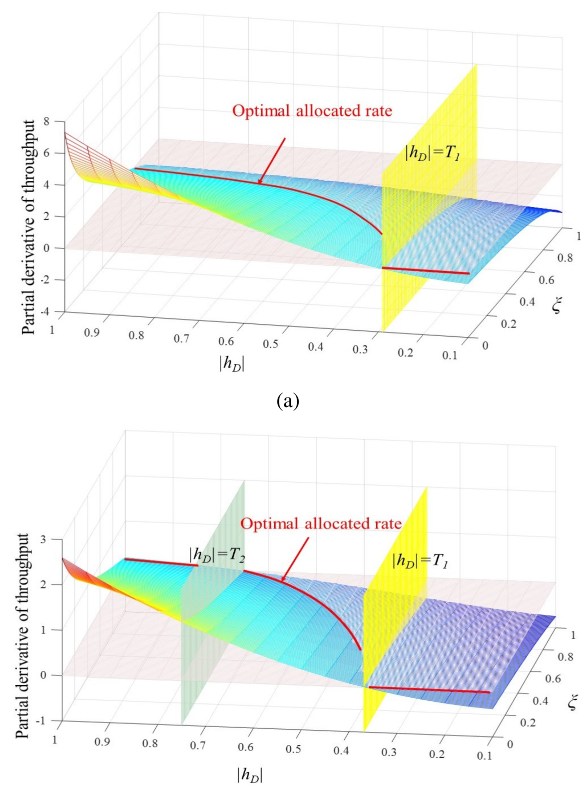

(a)

(b)

Fig. 3: Partial derivative of the underlay throughput under different conditions: (a) $\beta P_D\|h_{DBD}\|^2 > \sigma^2$ (b) $\beta P_D\|h_{DBD}\|^2 < \sigma^2$

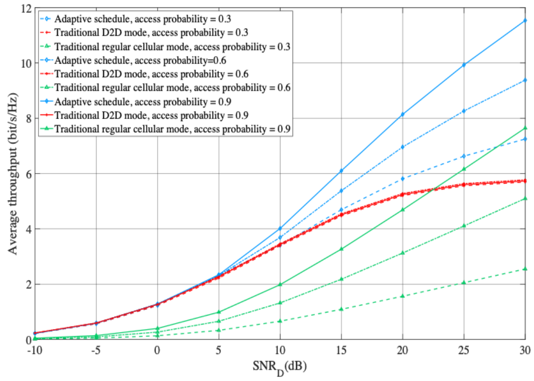

Fig. 4: Throughput performance comparison under different β

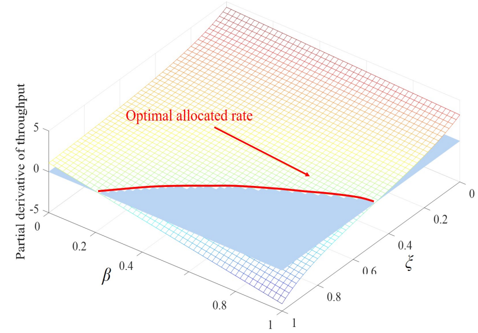

Fig. 5: Joint impact of β and ξ to the partial derivative of the underlay throughput

Remark 2: When $|h_D| < T_1$, $F(\xi, \beta, h_D)$ is smaller than 0 for all the allocated power rates. Here, $T_1 = \frac{\beta(P_C|g_{CD}|^2+\sigma^2)|h_{DBD}|^2}{\sigma^2+P_D|h_{DBD}|^2}$. Thus, the achievable throughput $u(\xi, \beta, h_D)$ is monotonically decreasing with respect to ξ and $\xi = 0$ is the optimal rate.

As intuitively anticipated, the above indicates that with deep channel fading, the D2D link brings no benefits, and CBS relay link should, instead, be used.

Remark 3: Under the condition that $\beta P_D|h_{DBD}|^2 > \sigma^2$ and $|h_D| > T_1$, or the condition that $\beta P_D|h_{DBD}|^2 < \sigma^2$ and $T_1 < |h_D| < T_2$, where $T_2 = \frac{\beta(P_C|g_{CD}|^2+\sigma^2)|h_{DBD}|^2}{\sigma^2-\beta P_D|h_{DBD}|^2}$, $F(\xi, \beta, h_D) > 0$ when ξ is smaller but decreases with increasing ξ. The intersection line of the partial derivative surface with the zero-flat corresponds to the optimal ξ maximizing $u(\xi, \beta, h_D)$.

Remark 4: Under the condition that $\beta P_D|h_{DBD}|^2 < \sigma^2$ and $|h_D| > T_2$, $F(\xi, \beta, h_D) > 0$ for all the allocated power rates. Thus, the achievable throughput $u(\xi, \beta, h_D)$ is monotonically increasing in ξ and $\xi = 1$ is the optimal rate.

We then evaluate the throughput performance under three underlay modes with different spectrum access rate for the relay link, i.e., $\beta = 0.9, 0.6$ and 0.3. It is shown in Fig. 4 that, with realistic time-varying D2D channel, the proposed scheduling is in general superior to other static scheduling which indicates the benefit provided by the developed adaptive switch scheduling. In addition, in high SNR region, the increasing performance of traditional underlay D2D mode saturates, since it is constrained by the interference from the CUE. When β increases, the performance gaps between the adaptive scheduling and D2D direct scheduling expand. It reveals that the D2D emitter needs to allocate less transmitter power via the D2D direct link. This conclusion can also be drawn from Fig. 5.

VI. Conclusions

In this paper, we considered the underlay D2D communication problem in dynamic wireless propagation environments and designed the adaptive switch scheduling which can jointly perform mode selection and power allocation. Particularly, we showed the selected mode and the optimal power allocation are closely related with dynamic channel gains. An adaptive switch scheduling with channel estimation algorithm was then developed. Simulation results were provided to validate the designed scheme, with which the significant improvement in throughput has been attained.

References

[1] D. Feng et al., "Device-to-device communications in cellular networks ", *IEEE Commun. Mag.*, vol. 52, no. 4, pp. 49-55, April 2014.

[2] D. Feng, et al., "Device-to-device communications underlaying cellular networks," *IEEE Trans. Commun.*, vol. 61, no. 8, pp. 3541-3551, Aug. 2013.

[3] M. Jung, K. Hwang, and S. Choi, "Joint mode selection and power allocation scheme for power-efficient device-to-device (D2D) communication," in *Proc. IEEE VTC-Spring*, Yokohama, Japan, May 2012, pp. 1-5.

[4] A. Tang, X. Wang, and C. Zhang, "Cooperative full duplex device to device communication underlaying cellular networks," *IEEE Wireless Commun.*, vol. 16, no. 12, pp. 7800–7815, Dec. 2017.

[5] J. Lee, and J. H. Lee, " Joint mode selection and resource allocation for relay-based D2D communications," *IEEE Commun. Lett.*, vol. 23, no. 5, pp. 909-912, May 2019.

[6] X. Q. Lin, J. G. Andrews, and A. Ghosh, "Spectrum sharing for device-to-device communication in cellular networks," *IEEE Trans. Wireless Commun.*, vol. 13, no. 12, pp. 6727-6740, Dec. 2014.

[7] C. Khirallah, D. Vukobratovic and J. Thompson, "Performance analysis and energy efficiency of random network coding in LTE-advanced," *IEEE Trans. Wireless Commun.*, vol. 11, no. 12, pp. 4275-4285, Dec. 2012.

[8] P. Sadeghi, R. Kennedy, P. Rapajic, and R. Shams, "Finite-state Markov modelling of fading channels: a survey of principles and applications," *IEEE Signal Process. Mag.*, vol. 25, no. 5, pp. 57-80, Aug. 2008.

[9] M. W. Sun, et al., "Adaptive sensing scheduling for dynamic spectrum sharing in time-varying channel," *IEEE Trans. Veh. Technol.*, vol. 67, no. 6, pp. 5520-5524, Jan. 2018.